Metabolomic Alterations in Mammary Glands from Pubertal Mice Fed a High-Fat Diet

Lin Yan, Bret M Rust, Sneha Sundaram and Michael R Bukowski

U.S. Department of Agriculture, Agricultural Research Service, Grand Forks Human Nutrition Research Center, Grand Forks, ND, USA.

Nutrition and Metabolic Insights
Volume 16: 1–10

DOI: 10.1177/11786388221148858
SAGE

ABSTRACT: Dietary malpractice is a risk factor for obesity. This study tested the hypothesis that consumption of a high-fat diet alters mammary metabolome in pubertal mice. We performed untargeted metabolomic analysis of primary metabolism on mammary glands from pubertal mice fed the AIN93G standard diet or a high-fat diet (HFD) for 3 weeks. We identified 97 metabolites for statistical comparisons. The HFD altered the amino acid metabolism considerably. This included elevated expression of branched-chain amino acids, non-essential amino acids (aspartic acid and glutamic acid), and methionine sulfoxide (oxidized methionine) and an alteration in the aminoacyl-tRNA biosynthesis pathway. Furthermore, elevations of fumaric acid and malic acid (both are citrate cycle intermediates) and glyceric acid (its phosphate derivatives are intermediates of glycolysis) in HFD-fed mice suggest an acceleration of both citrate cycle and glycolysis. Lower expression of glycerol, oleic acid, and palmitoleic acid, as well as decreased mammary expression of genes encoding lipid metabolism (*Acaca*, *Fads1*, *Fasn*, *Scd1*, and *Srebf1*) in HFD-fed mice indicate an attenuated lipid metabolism in the presence of adequate dietary fat. In conclusion, consumption of the HFD for 3 weeks alters metabolic profile of pubertal mammary glands. This alteration may affect mammary development and growth in pubertal mice.

KEYWORDS: Metabolome, mammary glands, puberty, diet, mice

RECEIVED: October 25, 2022. **ACCEPTED:** December 14, 2022.

TYPE: Original Research

FUNDING: The author(s) disclosed receipt of the following financial support for the research, authorship, and/or publication of this article: This work was funded by the USDA Agricultural Research Service Projects #3062-51000-050-446 00D and #3062-51000-056-00D.

DECLARATION OF CONFLICTING INTERESTS: The author(s) declared no potential conflicts of interest with respect to the research, authorship, and/or publication of this article.

CORRESPONDING AUTHOR: Lin Yan, USDA-ARS Grand Forks Human Nutrition Research Center, Grand Forks, ND 58203, USA. Email: lin.yan@usda.gov

Introduction

Childhood obesity has reached epidemic proportions worldwide.[1] It remains one of the most prevalent public health problems. Childhood obesity in girls is associated with an increased risk of breast cancer later in life. Studies have shown that obese girls exhibit an early onset of puberty[2,3] and breast development[4,5] with elevations of ovarian steroid hormones. Early menarche in girls is associated with an increased risk of adulthood breast cancer.[6-8]

Mammary gland development mainly occurs during puberty. With the onset of puberty, ductal morphogenesis creates epithelial mammary trees that fill the mammary fat pad. Ovary-derived steroid hormones, in addition to pituitary hormones, play important roles in the growth of pubertal mammary glands. Estrogen acts directly on mammary glands; estrogen receptor 1 regulates ductal morphogenesis[9,10] and estrogen receptor 2 facilitates terminal differentiations.[11] Obese girls with early onset of breast development have elevated estrogen in saliva compared to girls with normal body weights.[5] Laboratory studies have shown that higher concentrations of estrogen and its receptors occur in mammary glands from pubertal mice fed an obesogenic diet compared to those fed a standard control diet.[12]

Dietary malpractice is a risk factor for obesity. Feeding weanling mice a high-fat diet increases body fat mass,[13,14] disrupts the pattern of metabolism (eg, respiratory exchange ratio),[14] and changes plasma concentrations of cytokines that are involved in metabolism (eg, leptin and adiponectin).[13,14] Furthermore, the high-fat diet alters metabolic profile of mammary tumors[15] and enhances mammary tumorigenesis[16] in MMTV-PyMT mice. However, there is a lack of knowledge of the impact of dietary fat on pubertal mammary metabolism. We hypothesized that consumption of a high-fat diet alters mammary metabolome in pubertal mice. In this study, we performed an untargeted metabolomic analysis of primary metabolism on mammary glands from pubertal mice fed a high-fat diet in comparison to that from their age-matched counterparts fed the AIN93G standard diet.

Materials and Methods

Animals and diets

Three-week-old female C57BL/6NHsd mice (Envigo, Madison, WI, USA) were group-housed (3 per cage) in a pathogen-free room with a 12:12-hour light/dark cycle and a temperature of 22 ± 1°C. The standard AIN93G diet[17] and a high-fat diet (HFD) containing 16% and 45% of energy from soybean oil, respectively, were used in this study (Table 1). Diets (powder form) were kept at −20°C. Fresh diets were provided to mice every other day.

Experimental design

The study design was reported previously.[12] Briefly, mice were acclimated with the AIN93G diet for 2 days before they were randomly assigned to 2 groups of 70 each and fed the AIN93G diet or HFD and deionized water *ad libitum* for 3 weeks.

Table 1. Diet composition.

	AIN93G	HIGH-FAT
Ingredient	g/kg	g/kg
Corn starch	397.5	42.5
Casein	200	239.4
Dextrin	132	239.4
Sucrose	100	119.7
Soybean oil	70	239.4
Cellulose	50	59.8
AIN93 mineral mix	35	41.9
AIN93 vitamin mix	10	12
L-Cystine	3	3.6
Choline bitartrate	2.5	3
t-Butylhydroquinone	0.014	0.017
Total	1000	1000
Energy	%	%
Protein	20	20
Fat	16	45
Carbohydrate	64	35
Analyzed gross energy (kcal/g)[a]	4.3 ± 0.1	5.2 ± 0.1

[a]Quantified by using an oxygen bomb calorimeter, Model 6200 (Parr Instrument, Moline, IL, USA), n = 3 per diet (means ± SEM).

Mice were weighed weekly. At the end of study, 5 mice from each group were euthanized (intra-peritoneal injection of ketamine and xylazine) and followed by exsanguination every 4 hours at Zeitgeber time (ZT) 0, 4, 8, 12, 16, 20, and 24 over a period of 48 hours. Mammary glands were collected and stored at −80°C.

Metabolomic analysis

Twelve mammary samples from each group (harvested in the dark phase at ZT 16 and 20) were used for metabolomic analysis. The analysis[18,19] was performed at the West Coast Metabolomics Center (University of California-Davis, Davis, CA, USA). Briefly, mammary tissues were extracted by the acetonitrile/isopropanol/H_2O (3:3:2) buffer, resuspended in a diluted acetonitrile solution (acetonitrile/H_2O, 1:1), and analyzed by gas chromatography time-of-flight mass spectrometry (GC-TOF-MS) for untargeted metabolomics of primary metabolism. Obtained data were processed by using the BinBase database.[20] For identified compounds, quantifier ion peak heights were normalized to the sum intensities of all known compounds. Compounds representing less than 0.02% of total signal intensity were excluded from statistical analysis. Additional compounds were excluded from statistical analysis if they could not be identified as metabolites or metabolic intermediates common to mammalian metabolism based on the Kyoto Encyclopedia of Genes and Genomes (KEGG) database or the Human Metabolome database.[21-23]

RNA isolation and real-time quantitative PCR

Total RNA from mammary glands was isolated by using the QIAzol Lysis reagent following the protocol from RNeasy Lipid Tissue Mini Kit (Qiagen, Germantown, MD, USA). The quality and quantity of the RNA were analyzed by using the NanoDrop 8000 spectrophotometer (Thermo Scientific, Wilmington, DE, USA). cDNA was synthesized by using the high-capacity cDNA reverse transcription kit (Applied Biosystems, Waltham, MA, USA). Real-time qPCR of acetyl-CoA carboxylase (*Acaca*) (Mm01304257_m1), fatty acid desaturases (*Fads*) 1 (Mm00507605_m1) and 2 (Mm00517221_m1), fatty acid synthase (*Fasn*) (Mm00662319_m1), stearoyl-CoA desaturase 1 (*Scd1*) (Mm00772290_m1), and sterol regulatory element-binding protein 1 (*Srebf1*) (Mm00550338_m1) was analyzed and normalized to the 18 S rRNA (Mm03928990_g1) by using the TaqMan Assay of Demand primers on the ABI QuantStudio 12K-Flex Real-time PCR system (Applied Biosystems). The $2^{-\Delta\Delta CT}$ method was used to calculate the relative changes in gene expression.[24]

Statistical analyses

The GLM procedure was used to compare differences in metabolites between the AIN93G and HFD groups with the false discovery rate (FDR)-corrected *p* values (obtained by PROC MULTTEST) reported (SAS 9.4, SAS Institute, Cary, NC, USA). Student t-test was performed to compare differences in genes encoding lipid metabolism between the 2 groups (SAS 9.4). For metabolomic analysis, data were normalized by the Pareto scaling method and analyzed by sparse partial least square-discriminant analysis (sPLS-DA) (MetaboAnalyst 5.0, McGill University, Sainte Anne de Bellevue, Quebec, Canada).[25,26] Obtained results from the HFD group are reported as fold changes to that from the AIN93G group. Results are reported as means ± standard error of the mean (SEM); differences with a $P \leqslant .05$ are considered significant.

Pathway and network analyses were conducted by using MetaboAnalyst 5.0 (McGill University).[27] Pathway analysis of alterations in metabolic pathways by the HFD was performed by using the pathway library for *Mus musculus* according to the KEGG database.[28] Pathway enrichment analysis coupled with pathway topology analysis was conducted to identify the altered metabolic pathways with the Holm-adjusted *P* values reported.[29] Network analysis was performed to map the functional relationships of identified metabolites by using the KEGG global metabolic network and the metabolite-metabolite interaction network analyses. Differences with a $P \leqslant .05$ are considered significant.

Table 2. Identified metabolites related to amino acid metabolism in mammary glands from pubertal mice fed the AIN93G or high-fat diet.

	AIN93G	HIGH-FAT	*P*
Alanine	1 ± 0.05	0.99 ± 0.05	.98
α-Aminoadipic acid	1 ± 0.13	1.08 ± 0.06	.71
Asparagine	1 ± 0.08	1.33 ± 0.07	.04
Aspartic acid	1 ± 0.08	1.42 ± 0.12	.05
β-Alanine	1 ± 0.09	1.01 ± 0.09	.98
Citrulline	1 ± 0.07	1.24 ± 0.07	.10
Creatinine	1 ± 0.28	1.06 ± 0.13	.97
Cysteine	1 ± 0.12	1.00 ± 0.11	1.00
Glutamic acid	1 ± 0.06	1.37 ± 0.09	.03
Glutamine	1 ± 0.06	1.12 ± 0.07	.33
Glycine	1 ± 0.07	1.23 ± 0.09	.17
Hypotaurine	1 ± 0.14	0.38 ± 0.09	.02
Isoleucine	1 ± 0.07	1.41 ± 0.07	.01
Leucine	1 ± 0.04	1.40 ± 0.07	<.01
Lysine	1 ± 0.09	1.17 ± 0.10	.39
Methionine	1 ± 0.04	0.65 ± 0.12	.05
Methionine sulfoxide	1 ± 0.12	2.43 ± 0.31	.01
N-acetylaspartic acid	1 ± 0.08	1.15 ± 0.15	.57
Ornithine	1 ± 0.08	1.31 ± 0.07	.05
Oxoproline	1 ± 0.06	1.17 ± 0.08	.24
Phenylalanine	1 ± 0.07	1.32 ± 0.09	.05
Proline	1 ± 0.11	1.12 ± 0.11	.61
Serine	1 ± 0.04	1.11 ± 0.05	.21
Taurine	1 ± 0.07	0.84 ± 0.07	.29
Threonine	1 ± 0.06	1.01 ± 0.07	.98
Trans-4-hydroxyproline	1 ± 0.12	1.14 ± 0.13	.61
Tryptophan	1 ± 0.08	1.14 ± 0.13	.56
Tyrosine	1 ± 0.07	1.29 ± 0.06	.04
Urea	1 ± 0.06	1.14 ± 0.08	.33
Valine	1 ± 0.08	1.33 ± 0.08	.05

Values (means ± SEM) of the high-fat diet group are standardized to that of the AIN93G group (n = 12 per group). Differences at $P \leq .05$ are considered significant (FDR-adjusted *P* values).

Table 3. Identified metabolites related to lipid metabolism in mammary glands from pubertal mice fed the AIN93G or high-fat diet.

	AIN93G	HIGH-FAT	*P*
Arachidic acid	1 ± 0.07	0.97 ± 0.08	.94
Arachidonic acid	1 ± 0.09	0.65 ± 0.12	.12
Caproic acid	1 ± 0.13	1.57 ± 0.20	.10
Cholesterol	1 ± 0.06	0.97 ± 0.06	.91
Ethanolamine	1 ± 0.08	1.07 ± 0.06	.62
Glyceric acid	1 ± 0.09	1.59 ± 0.19	.05
Glycerol	1 ± 0.06	0.73 ± 0.04	.02
Glycerol-3-galactoside	1 ± 0.24	0.56 ± 0.12	.24
Inositol-4-monophosphate	1 ± 0.09	0.86 ± 0.10	.48
Lauric acid	1 ± 0.11	0.96 ± 0.06	.93
Linoleic acid	1 ± 0.16	0.75 ± 0.07	.31
1-Monoolein	1 ± 0.24	0.76 ± 0.18	.61
1-Monopalmitin	1 ± 0.09	0.86 ± 0.08	.43
2-Monoolein	1 ± 0.08	2.35 ± 0.91	.98
2-Monopalmitin	1 ± 0.28	0.58 ± 0.06	.31
Myristic acid	1 ± 0.08	0.77 ± 0.04	.09
Oleamide	1 ± 0.17	0.92 ± 0.17	.91
Oleic acid	1 ± 0.13	0.58 ± 0.06	.05
Palmitic acid	1 ± 0.08	0.82 ± 0.06	.23
Palmitoleic acid	1 ± 0.14	0.32 ± 0.03	<.01
Pentadecanoic acid	1 ± 0.08	1.09 ± 0.05	.56
Phosphate	1 ± 0.07	1.19 ± 0.10	.29
Phosphoethanolamine	1 ± 0.12	1.13 ± 0.12	.61
Stearic acid	1 ± 0.09	0.89 ± 0.09	.58
Zymosterol	1 ± 0.08	0.82 ± 0.09	.30

Values (means ± SEM) of the high-fat diet group are standardized to that of the AIN93G group (n = 12 per group). Differences at $P \leq .05$ are considered significant (FDR-adjusted *P* values).

Results

Metabolomic analysis

Feeding pubertal mice the HFD for 3 weeks resulted in a slight, but significant increase in body weight (19.0 ± 0.2 and 18.2 ± 0.2 g; $P < .05$, n = 70 per group).[12] We identified a total of 149 compounds from 361 discrete signals detected by GC-TOF-MS (Supplemental Table 1). Ninety-seven of the 149 compounds met the criteria for statistical analysis. They were grouped into 4 categories related to amino acid, lipid, energy, and nucleotide and vitamin metabolism (Tables 2–5). Twenty-two of the identified metabolites differed significantly between the AIN93G and HFD groups (Tables 2–5).

The hierarchical clustering heatmap analysis of the identified metabolites in mammary glands produced 2 responsive clusters of the 20 metabolites that differed significantly

Table 4. Identified metabolites related to energy metabolism in mammary glands from pubertal mice fed the AIN93G or high-fat diet.

	AIN93G	HIGH-FAT	*P*
1,5-Anhydroglucitol	1 ± 0.08	1.01 ± 0.08	.98
Citric acid	1 ± 0.14	1,14 ± 0.08	.58
Fructose	1 ± 0.12	1.16 ± 0.12	.56
Fructose-6-phosphate	1 ± 0.28	1.05 ± 0.14	.98
Fumaric acid	1 ± 0.16	1.49 ± 0.07	.05
Glucose	1 ± 0.13	1.60 ± 0.25	.15
Glucose-6-phosphate	1 ± 0.30	1.02 ± 0.15	.98
Glutathione	1 ± 0.08	1.04 ± 0.09	.91
Glycerol-α-phosphate	1 ± 0.06	1.21 ± 0.12	.30
2-Hydroxyglutaric acid	1 ± 0.11	1.20 ± 0.09	.33
3-Hydroxybutyric acid	1 ± 0.17	1.32 ± 0.20	.43
Lactic acid	1 ± 0.09	0.91 ± 0.08	.61
Lactose	1 ± 0.12	0.59 ± 0.08	.05
Malic acid	1 ± 0.19	1.71 ± 0.10	.03
Maltose	1 ± 0.33	0.36 ± 0.13	.24
Maltotriose	1 ± 0.40	0.14 ± 0.07	.16
Mannose	1 ± 0.11	1.46 ± 0.19	.14
N-acetylmannosamine	1 ± 0.09	1.04 ± 0.07	.91
Pyruvic acid	1 ± 0.09	0.88 ± 0.12	.61
Sorbitol	1 ± 0.13	0.85 ± 0.12	.58
Succinic acid	1 ± 0.09	0.97 ± 0.10	.94
UDP-glucuronic acid	1 ± 0.07	0.98 ± 0.04	.94

Values (means ± SEM) of the high-fat diet group are standardized to that of the AIN93G group (n = 12 per group). Differences at $P \leq .05$ are considered significant (FDR-adjusted *P* values).

Table 5. Identified metabolites related to nucleotide and vitamin metabolism in mammary glands from pubertal mice fed the AIN93G or high-fat diet.

	AIN93G	HIGH-FAT	*P*
Nucleotides			
Adenine	1 ± 0.07	1.01 ± 0.05	.98
Adenosine	1 ± 0.15	1.14 ± 0.13	.61
Adenosine-5-monophosphate	1 ± 0.13	0.59 ± 0.13	.12
Hypoxanthine	1 ± 0.11	1.42 ± 0.17	.13
Inosine	1 ± 0.10	1.31 ± 0.15	.24
Inosine 5-monophosphate	1 ± 0.12	0.62 ± 0.16	.20
N-methyl-UMP	1 ± 0.09	1.01 ± 0.13	.98
Parabanic acid	1 ± 0.09	1.02 ± 0.05	.94
Pyrophosphate	1 ± 0.10	0.74 ± 0.08	.16
Ribose	1 ± 0.07	1.35 ± 0.12	.08
Thymidine	1 ± 0.12	0.86 ± 0.07	.56
Uracil	1 ± 0.07	1.41 ± 0.13	.05
Uric acid	1 ± 0.09	0.82 ± 0.05	.20
Uridine	1 ± 0.06	1.54 ± 0.21	.09
Xanthine	1 ± 0.06	1.45 ± 0.14	.05
Vitamins			
Dehydroascorbic acid	1 ± 0.06	0.90 ± 0.06	.45
Nicotinamide	1 ± 0.11	1.00 ± 0.09	.99
Pantothenic acid	1 ± 0.08	0.87 ± 0.07	.43
Threonic acid	1 ± 0.11	1.31 ± 0.15	.24
α-Tocopherol	1 ± 0.16	0.44 ± 0.03	.03

Abbreviation: N-methyl-UMP, N-methyl-uridine-5-monophosphate.
Values (means ± SEM) of the high-fat diet group are standardized to that of the AIN93G group (n = 12 per group). Differences at $P \leq .05$ are considered significant (FDR-adjusted *P* values).

between the 2 groups (Figure 1). The expression of 7 metabolites was lower in HFD-fed mice than in AIN93G-fed mice. These included oleic acid (18:1), palmitoleic acid (16:1), hypotaurine, methionine, lactose, glycerol, and α-tocopherol. The expression of 13 metabolites was higher in the HFD-fed mice. These included fumaric acid, uracil, ornithine, asparagine, methionine sulfoxide, malic acid, valine, xanthine, glyceric acid, tyrosine, glutamic acid, leucine, and isoleucine.

The sPLS-DA scores plot showed a clear separation between the AIN93G and HFD groups (Figure 2A). The loadings plot for component 1 showed that amino acids and amino acid metabolites (leucine, methionine sulfoxide, isoleucine, glutamic acid, hypotaurine, and tyrosine), lipid metabolites palmitoleic acid (16:1) and glycerol, the citrate cycle intermediate malic acid, and vitamin α-tocopherol are major determinants of separation (Figure 2B).

The loadings plot for component 2 demonstrated that metabolites related to energy metabolism (maltotriose, 2-hydtoxyglutaric acid, 1,5-anhydroglucitol, succinic acid, and maltose), amino acids (threonine, asparagine, and lysine), nucleotide adenine, and fatty acid linoleic acid (18:2) were major determinants of separation (Figure 2C).

The loadings plot for component 3 showed that lipid metabolites (lauric acid, ethanolamine, and myristic acid), metabolites related to energy metabolism (3-hydroxybutyric acid, N-acetylmannosamine, citric acid, and sorbitol), amino

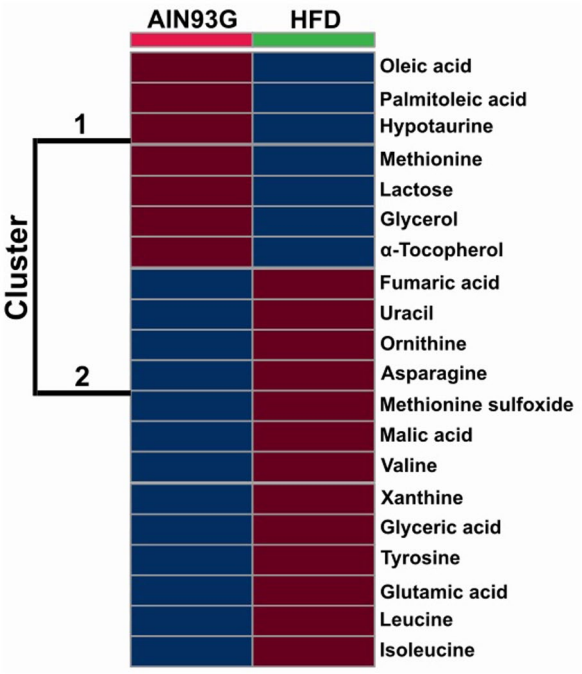

Figure 1. Hierarchical clustering heatmap of the 20 metabolites in mammary glands that differed significantly between the AIN93G-fed and high-fat diet (HFD)-fed pubertal mice ($P < .05$ with applied FDR). Heatmap squares represent the mean of 12 samples. The red color indicates greater signal strength and blue color indicates weaker signal strength by GC-TOF-MS.

acid metabolites lysine and β-alanine, and nucleotide adenosine-5-monophosphate were major determinants of separation (Figure 2D).

Pathway analysis

The pathway analysis examined alterations in metabolic pathways by the HFD. It mapped the identified metabolites into 57 metabolic pathways (Supplemental Table 2) based on the KEGG database.[22,28] Five pathways were altered significantly by the HFD (Figure 3 and Table 6). These pathways included aminoacyl-tRNA biosynthesis, alanine, aspartate, and glutamate metabolism, arginine biosynthesis, pantothenate and CoA biosynthesis, and branched-chain amino acid (BCAA, valine, leucine, and isoleucine) biosynthesis.

Network analyses

The KEGG global metabolic network analysis identified 31 metabolic pathways that were altered by the HFD (Supplemental Table 3). Among them, 6 were altered significantly (Table 6). These included aminoacyl-tRNA biosynthesis, arginine biosynthesis, BCAA biosynthesis, alanine, aspartate, and glutamate metabolism, pantothenate and CoA biosynthesis, and glycerolipid metabolism. The metabolite-metabolite interaction network analysis showed the functional relationship of the identified metabolites (Figure 4).

Expression of genes encoding lipid metabolism

The HFD, compared to the AIN93G diet, decreased mammary expression of genes encoding enzymes that are involved in lipid metabolism. These genes were *Acaca*, *Fads1*, *Fasn*, *Scd1*, and *Srebf1* (Table 7). There was no significant difference in *Fads2* between the 2 groups (Table 7).

Discussion

The present study showed that consumption of an HFD for 3 weeks altered metabolomic profile of mammary glands in pubertal mice.

Both pathway and network analyses showed that 4 of the metabolic pathways that were significantly altered by the HFD were related to amino acid metabolism. The aminoacyl-tRNA biosynthesis pathway is important in protein synthesis.[30] It is a group of aminoacyl-tRNA synthetases that catalyze aminoacylations by covalently linking an amino acid to its cognate tRNA in the first step of protein translation. The other 3 pathways are alanine, aspartate, and glutamate metabolism, arginine biosynthesis, and BCAA biosynthesis pathways.

The alteration of the BCAA biosynthesis pathway is supported by elevations of isoleucine, leucine, and valine in mammary glands from mice fed the HFD. BCAAs account for one-third of dietary essential amino acids.[31] They activate mammalian target of rapamycin complex (mTORC1) signaling pathway, which is essential for initiation of protein synthesis.[32,33] The BCAAs increase protein synthesis in lactating mammary glands[34] and breast cancer tissue[35] through the activation of mTORC1 signaling pathway. Increases of BCAAs in bloodstream occur in human obese subjects,[36,37] indicating abnormalities in BCAA metabolism in obesity. Findings from our study suggest that the HFD may impair BCAA metabolism or utilization in pubertal mammary glands.

The observed elevations of aspartic acid and glutamic acid in mammary glands and the alteration of the alanine, aspartate, and glutamate metabolism pathway by the HFD suggest an increase in biosynthesis of non-essential amino acids in pubertal mammary glands. These changes may be related to the altered BCAA metabolism. BCAAs are an indirect source of nitrogen for non-essential amino acid synthesis in mitochondria through α-ketoglutarate, a citrate cycle intermediate.[38,39] BCAAs interact with α-ketoglutarate to form glutamate, which in turn interacts with oxaloacetate to form aspartate and α-ketoglutarate.

Observations of decreased mammary expression of methionine and increased expression of methionine sulfoxide in HFD-fed mice indicate alterations in methionine metabolism. Methionine sulfoxide is the oxidized form of methionine; this oxidation can be reversed by methionine sulfoxide

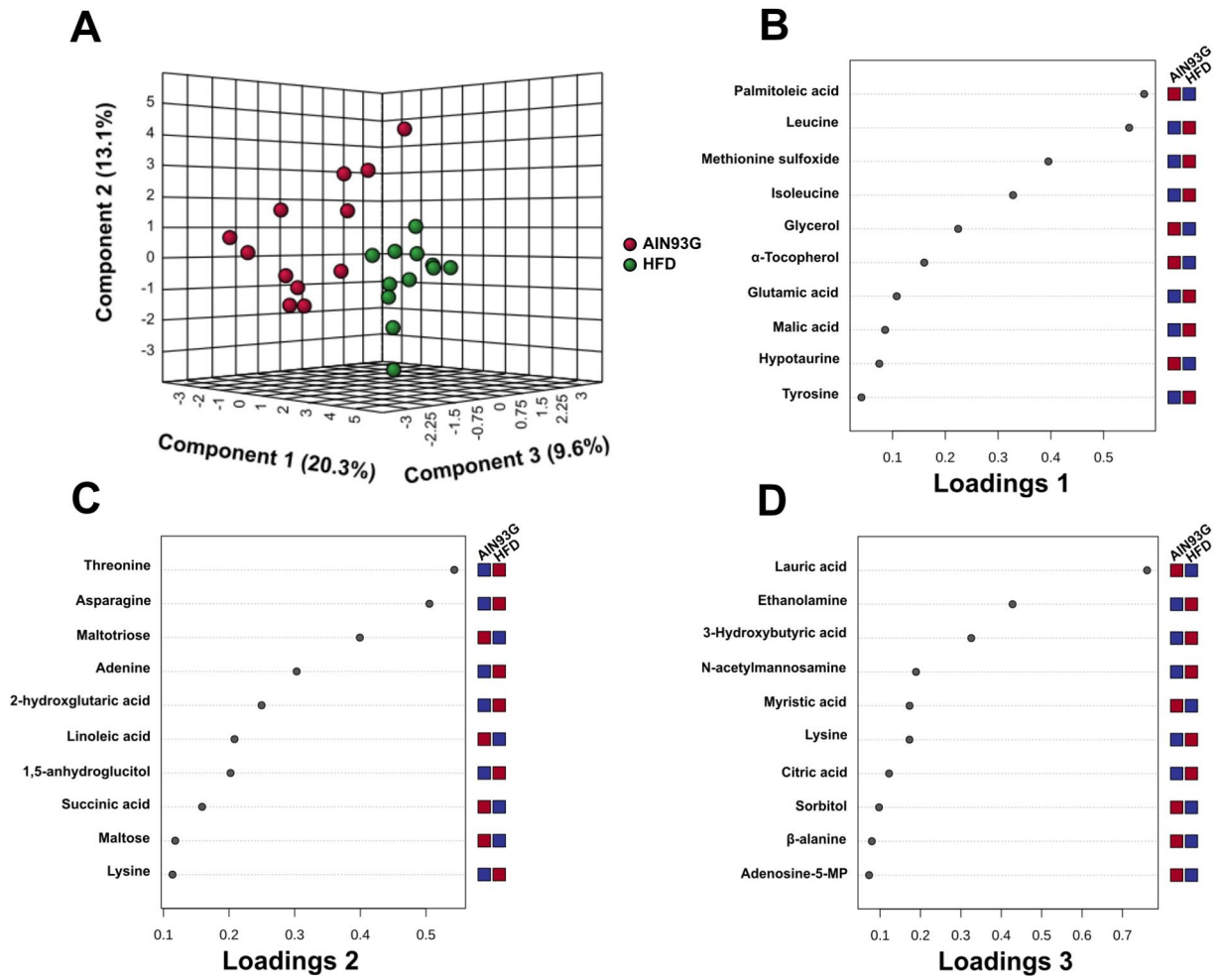

Figure 2. The scores plot by the sparse partial least square discriminant analysis (sPLS-DA) of mammary metabolites (A) and loadings plots of the 10 metabolites that are most influential in treatment separation between the AIN93G and high-fat diet groups for components 1 (B), 2 (C), and 3 (D) (n = 12 per group). The *x*-axis shows that variables are ranked by the absolute values of their loadings. The red color indicates greater signal strength and blue color indicates weaker signal strength by GC-TOF-MS. Adnosine-5-MP, adenosine-5-monophosphate.

reductases (Msr).[40] Increases in methionine sulfoxide have been associated with breast cancer development in in vitro and animal studies. For example, silencing MsrA in MDA-MB-231 breast cancer cells increases cell proliferation and extracellular matrix degradation and consequently results in more aggressive phenotype in nude mice.[41] High levels of MsrB1 transcript and promoter activity occur in lower metastatic MCP7 breast cancer cells, whereas low levels of both occur in high metastatic MDA-MB-231 cells.[42] Furthermore, the catabolism of methionine is linked to that of BCAAs through branched-chain keto-acid dehydrogenase.[43] Thus, the observed elevation of BCAAs by the HFD may be interrelated with the lower expression of methionine, as methionine-sparing effect of BCAAs has been reported in animal studies.[44]

Greater mammary expression of fumaric acid and malic acid occurred in HFD-fed mice than in their AIN93G-fed counterparts. Furthermore, the HFD increased glyceric acid and decreased glycerol in mammary glands. Both fumarate and malate are intermediates of the citrate cycle. Glyceric acid is an oxidative product of glycerol. Several phosphate derivatives of glyceric acid are important intermediates of glycolysis (eg, 1,3-biphosphoglycerate). These findings suggest that the HFD may have facilitated anabolic processes through both citrate cycle and glycolysis to supply ATP to pubertal mammary glands.

The mammary expression of genes encoding fatty acid and triacylglycerol metabolism (*Acaca*, *Fads1*, *Fasn*, *Scd1*, and *Srebf1*) was lower in HFD-fed mice than in AIN93G-fed controls. Furthermore, oleic acid, palmitoleic acid, and glycerol were lower in mammary glands from HFD-fed mice. Oleate and palmitoleate are metabolic products of stearoyl-CoA desaturase 1 (encoded by *Scd1*) from stearoyl-CoA and palmitoyl-CoA, respectively. Glycerol provides the carbon backbone for synthesis of triacylglycerols, which is catalyzed by sterol regulatory element-binding transcription factor 1 (encoded by *Srebf1*). Our findings suggest that the HFD may have satisfied the anabolic need for lipids by providing adequate fatty acids from the digested triacylglycerols, which attenuates de novo lipid synthesis in pubertal mammary glands.

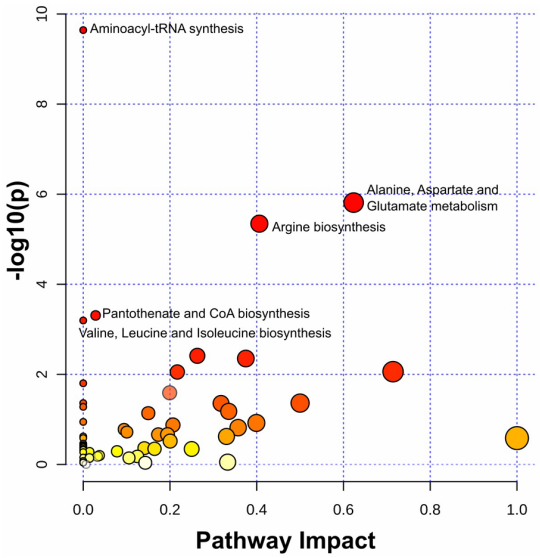

Figure 3. Metabolic pathways from identified metabolites in mammary glands from pubertal mice fed the AIN93G or high-fat diet (n = 12 per group). Each node represents a pathway. The nodes with larger sizes and darker color (from white-yellow to red) positioning toward the top right region represent greater pathway impact values and pathway enrichment. Pathways that are altered significantly are presented with their names next to their nodes. All metabolic pathways identified in this study are available in Supplemental Table 2.

Table 6. Metabolic pathways identified by the pathway analysis and network analysis that are significantly altered by the high-fat diet.

PATHWAYS (BY PATHWAY ANALYSIS)	MATCH STATUS[a]	P[b]	IMPACT[c]
Aminoacyl-tRNA biosynthesis	17/48	<.01	0
Alanine, aspartate, and glutamate metabolism	10/28	<.01	0.62
Arginine biosynthesis	7/14	<.01	0.41
Pantothenate and CoA biosynthesis	6/19	.04	0.03
Valine, leucine, and isoleucine biosynthesis	4/8	.05	0
PATHWAYS (BY KEGG GLOBAL METABOLIC NETWORK ANALYSIS)	**MATCH STATUS[d]**	***P*[e]**	
Aminoacyl-tRNA biosynthesis	8/22	<.01	
Arginine biosynthesis	4/14	<.01	
Valine, leucine, and isoleucine biosynthesis	3/8	<.01	
Alanine, aspartate, and glutamate metabolism	4/28	<.01	
Pantothenate and CoA biosynthesis	3/17	.02	
Glycerolipid metabolism	2/7	.04	

[a]Number of identified metabolites that match to pathway metabolites (calculation based on total number of metabolites identified in this study).
[b]Obtained by the over-representation analysis and adjusted by the Holm method.
[c]Obtained by the pathway topology analysis.
[d]Number of identified metabolites that match to pathway metabolites (calculation based on the number of identified metabolites that differ significantly between the AIN93G and high-fat groups).
[e]False discovery rate-adjusted *P* values.

The finding of lactose in pubertal mammary glands was unexpected. Lactose is the primary carbohydrate in milk. Its synthesis is catalyzed by lactose synthetase in mammary epithelial cells during late pregnancy and lactation. Pubertal mammary development undergoes hormonal regulation. Puberty initiates branching morphogenesis, which requires growth hormone and estrogen to create ductal trees that fill the fat pad.[45] The AIN93G diet is formulated for growth, pregnancy, and lactation for rats and mice.[17] It conforms to or exceeds the nutrient requirements for laboratory rodents set forth by the National Research Council.[17] We quantified estrogen, progesterone, and their receptors in mammary glands from these pubertal mice.[12] Our findings suggest that the AIN93G formulation may play a role in ovary steroid hormone-mediated regulation in pubertal mammary development, which may be responsible, at least partly, for the lactose found in pubertal mammary glands.

Both lactose and glycerol (an alternative source of carbon for lactose synthesis) in mammary glands were lower in HFD-fed mice than in AIN93G-fed controls. This observation suggests that the HFD may have disturbed the mechanism through which the AIN93G diet elevated lactose in pubertal mammary glands. However, higher mammary concentrations of estrogen and estrogen receptor 1 occur in these HFD-fed pubertal mice.[12] Thus, the roles of the HFD-mediated elevation of ovary steroid hormones in pubertal mammary development, particularly that related to lactose production, warrant further investigation.

Mammary expression of α-tocopherol in HFD-fed mice was lower than that in AIN93G-fed mice. α-Tocopherol protects polyunsaturated fatty acids in cell membranes and lipoproteins against oxidation. Intestinal absorption α-tocopherol depends on the quantity of fat in a diet. Tissue storage of α-tocopherol relies on α-tocopherol transfer protein[46,47] and tocopherol-associated protein[48] to transfer α-tocopherol between membranes. Catabolism of α-tocopherol is initiated by cytochrome P450 4F2/cytochrome P450 3A4.[49] The lower mammary α-tocopherol in HFD-fed mice does not seem to be due to a decrease in intestinal absorption because the HFD is a lipid-rich diet and soybean oil is a good source of α-tocopherol.[50] Rather, it may be related to a decrease in transport, an increase in catabolism, or both. α-Tocopherol reduces cell proliferation by inactivating protein kinase C in different cell types.[51,52] Thus, the impact of the HFD-mediated alteration in α-tocopherol metabolism on pubertal mammary development remains an interest for further investigation.

Laboratory rodents are nocturnal animals. They are active in the dark phase of the day (ZT 12-24). In a recent

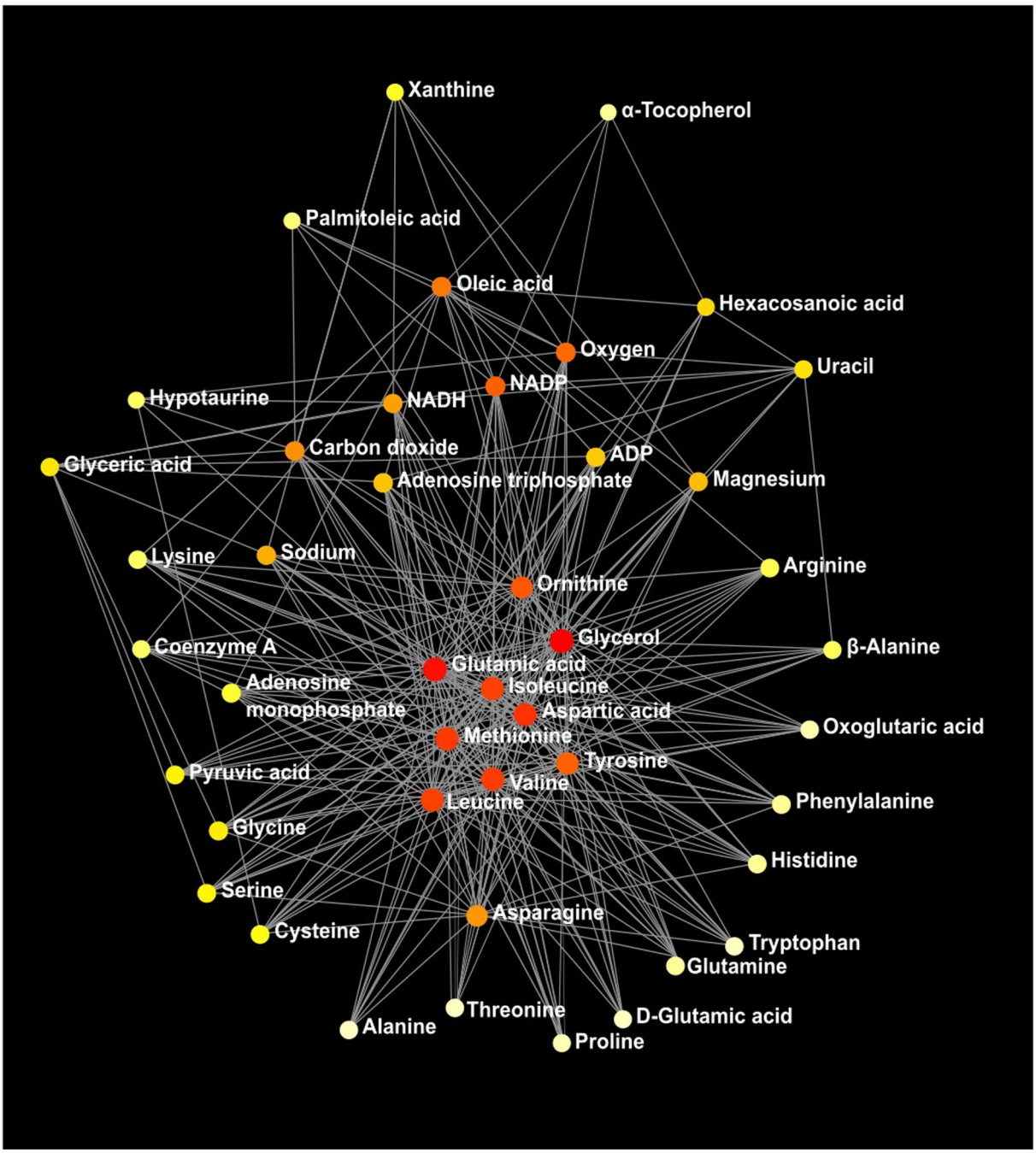

Figure 4. Metabolic network of identified metabolites in mammary glands from pubertal mice fed the AIN93G or high-fat diet (n = 12 per group). Colors (from white-yellow to red) represent levels of impact the metabolites have to the network in an ascending order (the number of connections a node has to other nodes and the number of shortest paths going through the node).

transcriptome analysis of liver samples from these pubertal mice, we found that the HFD-fed mice, compared to the AIN93G-fed controls, had greater numbers of differentially expressed genes and KEGG metabolic signaling pathways in the dark phase (particularly ZT 16-20) and fewer numbers in the light phase.[53] The present metabolomic analysis was performed by using mammary samples collected during the dark phase (ZT 16-20). Taken together with results from the transcriptome analysis, our findings indicate that the HFD alters metabolism of nocturnal rodents the most in the dark phase.

In conclusion, feeding pubertal mice the HFD for 3 weeks alters metabolic profile of mammary glands, with considerable alteration in amino acid metabolism. This alteration may affect mammary development and growth in pubertal mice. The impact of this metabolomic alteration by the HFD on breast health in adult ages remains an interest for further investigation.

Table 7. Expression of genes encoding enzymes involved in lipid metabolism in mammary glands from pubertal mice fed the AIN93G or high-fat diet.

	AIN93G	HIGH-FAT	*P*
Acaca	1 ± 0.18	0.41 ± 0.04	.01
Fads1	1 ± 0.15	0.62 ± 0.07	.03
Fads2	1 ± 0.15	0.81 ± 0.07	.27
Fasn	1 ± 0.21	0.36 ± 0.04	.01
Scd1	1 ± 0.14	0.29 ± 0.04	<.01
Srebf1	1 ± 0.12	0.68 ± 0.08	.04

Values are means ± SEM (n = 12 per group).

Acknowledgments

The authors gratefully acknowledge Dr. Kathleen Yeater (Plains Area Administrative Office, Agricultural Research Service) and Daniel Palmer for assistance in statistical analyses and the assistance from Lana DeMars and Jack He for technical support and vivarium staff for preparing experimental diets and providing high-quality animal care. USDA is an equal opportunity provider and employer. Mention of trade names or commercial products in this publication is solely for the purpose of providing specific information and does not imply recommendation or endorsement by the USDA.

Author Contributions

LY and SS designed the study, conducted experiments, collected data, and wrote the manuscript. All authors contributed to result interpretation and manuscript revision.

Ethics Statement

The Institutional Animal Care and Use Committee of the Grand Forks Human Nutrition Research Center approved this study.

Supplemental Material

Supplemental material for this article is available online.

REFERENCES

1. GBD 2015 Obesity Collaborators; Afshin A, Forouzanfar MH, et al. Health effects of overweight and obesity in 195 countries over 25 years. *New Engl J Med*. 2017;377:13-27.
2. Li W, Liu Q, Deng X, Chen Y, Liu S, Story M. Association between obesity and puberty timing: a systematic review and meta-analysis. *Int J Environ Res Public Health*. 2017;14:1266.
3. He F, Guan P, Liu Q, Crabtree D, Peng L, Wang H. The relationship between obesity and body compositions with respect to the timing of puberty in Chongqing adolescents: a cross-sectional study. *BMC Public Health*. 2017;17:664.
4. Rosenfield RL, Lipton RB, Drum ML. Thelarche, pubarche, and menarche attainment in children with normal and elevated body mass index. *Pediatrics*. 2009;123:84-88.
5. Zhai L, Liu J, Zhao J, et al. Association of obesity with onset of puberty and sex hormones in Chinese girls: a 4-year longitudinal study. *PLoS One*. 2015;10:e0134656.
6. Peeters PH, Verbeek AL, Krol A, Matthyssen MM, de Waard F. Age at menarche and breast cancer risk in nulliparous women. *Breast Cancer Res Treat*. 1995;33:55-61.
7. Lee SY, Kim MT, Kim SW, Song MS, Yoon SJ. Effect of lifetime lactation on breast cancer risk: a Korean women's cohort study. *Int J Cancer*. 2003;105:390-393.
8. Velie EM, Nechuta S, Osuch JR. Lifetime reproductive and anthropometric risk factors for breast cancer in postmenopausal women. *Breast Dis*. 2005-2006;24:17-35.
9. Bordini B, Rosenfield RL. Normal pubertal development: part I: the endocrine basis of puberty. *Pediatr Rev*. 2011;32:223-229.
10. Korach KS, Couse JF, Curtis SW, et al. Estrogen receptor gene disruption: molecular characterization and experimental and clinical phenotypes. *Recent Prog Horm Res*. 1996;51:159-186; discussion 186-188.
11. Förster C, Mäkela S, Wärri A, et al. Involvement of estrogen receptor beta in terminal differentiation of mammary gland epithelium. *Proc Natl Acad Sci U S A*. 2002;99:15578-15583.
12. Sundaram S, Johnson LK, Yan L. High-Fat diet alters circadian rhythms in mammary glands of pubertal mice. *Front Endocrinol*. 2020;11:349.
13. Sundaram S, Bukowski MR, Lie WR, Picklo MJ, Yan L. High-fat diets containing different amounts of n3 and n6 polyunsaturated fatty acids modulate inflammatory cytokine production in mice. *Lipids*. 2016;51:571-582.
14. Sundaram S, Yan L. Time-restricted feeding reduces adiposity in mice fed a high-fat diet. *Nutr Res*. 2016;36:603-611.
15. Yan L, Sundaram S, Rust BM, Picklo MJ, Bukowski MR. Metabolome of mammary tumors differs from normal mammary glands but is not altered by time-restricted feeding under obesogenic conditions. *Anticancer Res*. 2020;40:3697-3705.
16. Sundaram S, Yan L. High-fat diet enhances mammary tumorigenesis and pulmonary metastasis and alters inflammatory and angiogenic profiles in MMTV-PyMT mice. *Anticancer Res*. 2016;36:6279-6287.
17. Reeves PG, Nielsen FH, Fahey GC. AIN-93 purified diets for laboratory rodents: final report of the American Institute of Nutrition ad hoc Writing Committee on the reformulation of the AIN-76A rodent diet. *J Nutr*. 1993;123:1939-1951.
18. Fiehn O, Garvey WT, Newman JW, Lok KH, Hoppel CL, Adams SH. Plasma metabolomic profiles reflective of glucose homeostasis in non-diabetic and type 2 diabetic obese African-American women. *PLoS One*. 2010;5:e15234.
19. Piccolo BD, Keim NL, Fiehn O, Adams SH, Van Loan MD, Newman JW. Habitual physical activity and plasma metabolomic patterns distinguish individuals with low vs. High weight loss during controlled energy restriction. *J Nutr*. 2015;145:681-690.
20. Fiehn O, Wohlgemuth G, Scholz C. Setup and annotation of metabolomic experiments by integrating biological and mass spectrometric metadata. In: Ludäscher B, Raschid L, eds. *Data Integration in the Life Sciences*. Springer; 2005;224-239.
21. Kanehisa M. Toward understanding the origin and evolution of cellular organisms. *Protein Sci*. 2019;28:1947-1951.
22. Kanehisa M, Goto S. KEGG: kyoto encyclopedia of genes and genomes. *Nucleic Acids Res*. 2000;28:27-30.
23. Wishart DS, Feunang YD, Marcu A, et al. HMDB 4.0: the human metabolome database for 2018. *Nucleic Acids Res*. 2018;46:D608-D617.
24. Livak KJ, Schmittgen TD. Analysis of relative gene expression data using real-time quantitative PCR and the 2(-Delta delta C(T)) method. *Methods*. 2001;25:402-408.
25. Xia J, Wishart DS. Using MetaboAnalyst 3.0 for comprehensive metabolomics data analysis. *Curr Protoc Bioinformatics*. 2016;55:14.10.1-14.10.91.
26. van den Berg RA, Hoefsloot HC, Westerhuis JA, Smilde AK, van der Werf MJ. Centering, scaling, and transformations: improving the biological information content of metabolomics data. *BMC Genomics*. 2006;7:142.
27. Xia J, Wishart DS. MetPA: a web-based metabolomics tool for pathway analysis and visualization. *Bioinformatics*. 2010;26:2342-2344.
28. Kanehisa M, Furumichi M, Tanabe M, Sato Y, Morishima K. KEGG: new perspectives on genomes, pathways, diseases and drugs. *Nucleic Acids Res*. 2017;45:D353-D361.
29. Holm SA. A simple sequentially rejective multiple test procedure. *Scand J Stat*. 1979;6:65-70.
30. Rubio Gomez MA, Ibba M. Aminoacyl-TRNA synthetases. *RNA*. 2020;26:910-936.
31. Harper AE, Miller RH, Block KP. Branched-chain amino acid metabolism. *Annu Rev Nutr*. 1984;4:409-454.
32. Hong SO, Layman DK. Effects of leucine on in vitro protein synthesis and degradation in rat skeletal muscles. *J Nutr*. 1984;114:1204-1212.
33. Wolfson RL, Chantranupong L, Saxton RA, et al. Sestrin2 is a leucine sensor for the mTORC1 pathway. *Science*. 2016;351:43-48.

34. Rezaei R, Wu Z, Hou Y, Bazer FW, Wu G. Amino acids and mammary gland development: nutritional implications for milk production and neonatal growth. *J Anim Sci Biotechnol*. 2016;7:20.
35. Zhang L, Han J. Branched-chain amino acid transaminase 1 (BCAT1) promotes the growth of breast cancer cells through improving mTOR-mediated mitochondrial biogenesis and function. *Biochem Biophys Res Commun*. 2017;486:224-231.
36. Lackey DE, Lynch CJ, Olson KC, et al. Regulation of adipose branched-chain amino acid catabolism enzyme expression and cross-adipose amino acid flux in human obesity. *Am J Physiol Endocrinol Metab*. 2013;304:E1175-E1187.
37. She P, Van Horn C, Reid T, Hutson SM, Cooney RN, Lynch CJ. Obesity-related elevations in plasma leucine are associated with alterations in enzymes involved in branched-chain amino acid metabolism. *Am J Physiol Endocrinol Metab*. 2007;293:E1552-E1563.
38. Mayers JR, Torrence ME, Danai LV, et al. Tissue of origin dictates branched-chain amino acid metabolism in mutant Kras-driven cancers. *Science*. 2016;353:1161-1165.
39. Ananieva EA, Wilkinson AC. Branched-chain amino acid metabolism in cancer. *Curr Opin Clin Nutr Metab Care*. 2018;21:64-70.
40. Lee BC, Dikiy A, Kim HY, Gladyshev VN. Functions and evolution of selenoprotein methionine sulfoxide reductases. *Biochim Biophys Acta*. 2009;1790:1471-1477.
41. De Luca A, Sanna F, Sallese M, et al. Methionine sulfoxide reductase A down-regulation in human breast cancer cells results in a more aggressive phenotype. *Proc Natl Acad Sci U S A*. 2010;107:18628-18633.
42. De Luca A, Sacchetta P, Nieddu M, Di Ilio C, Favaloro B. Important roles of multiple sp1 binding sites and epigenetic modifications in the regulation of the methionine sulfoxide reductase B1 (MsrB1) promoter. *BMC Mol Biol*. 2007;8:39.
43. Benevenga NJ. Evidence for alternative pathways of methionine catabolism. *Adv Nutr Res*. 1984;6:1-18.
44. Langer S, Fuller MF. Interactions among the branched-chain amino acids and their effects on methionine utilization in growing pigs: effects on nitrogen retention and amino acid utilization. *Br J Nutr*. 2000;83:43-48.
45. Macias H, Hinck L. Mammary gland development. *Wiley Interdiscip Rev Dev Biol*. 2012;1:533-557.
46. Catignani GL. An alpha-tocopherol binding protein in rat liver cytoplasm. *Biochem Biophys Res Commun*. 1975;67:66-72.
47. Gohil K, Godzdanker R, O'Roark E, et al. Alpha-tocopherol transfer protein deficiency in mice causes multi-organ deregulation of gene networks and behavioral deficits with age. *Ann N Y Acad Sci*. 2004;1031:109-126.
48. Yamauchi J, Iwamoto T, Kida S, Masushige S, Yamada K, Esashi T. Tocopherol-associated protein is a ligand-dependent transcriptional activator. *Biochem Biophys Res Commun*. 2001;285:295-299.
49. Sontag TJ, Parker RS. Cytochrome P450 omega-hydroxylase pathway of tocopherol catabolism. Novel mechanism of regulation of vitamin E status. *J Biol Chem*. 2002;277:25290-25296.
50. U.S. Department of Agriculture ARS. FoodData Central: soybean oil. Accessed November 29, 2022. https://fdc.nal.usda.gov/fdc-app.html#/food-details/748366/nutrients
51. Tasinato A, Boscoboinik D, Bartoli GM, Maroni P, Azzi A. d-alpha-tocopherol inhibition of vascular smooth muscle cell proliferation occurs at physiological concentrations, correlates with protein kinase C inhibition, and is independent of its antioxidant properties. *Proc Natl Acad Sci U S A*. 1995;92:12190-12194.
52. Ricciarelli R, Tasinato A, Clément S, Ozer NK, Boscoboinik D, Azzi A. Alpha-tocopherol specifically inactivates cellular protein kinase C alpha by changing its phosphorylation state. *Biochem J*. 1998;334(Pt 1):243-249.
53. Yan L, Sundaram S, Rust BM, Palmer DG, Johnson LK, Zeng H. Consumption of a high-fat diet alters transcriptional rhythmicity in liver from pubertal mice. *Front Nutr*. 2023;9:1068350.